J IRAN CHEM SOC
DOI 10.1007/s13738-015-0652-6

ORIGINAL PAPER

Synthesis and heterogeneous catalytic activity of covalently immobilized hexamine cation as a magnetically-recoverable nanocatalyst

Sahar Kangari[1] · Issa Yavari[1] · Bakhshali Maasoumi[2]

Received: 10 December 2014 / Accepted: 25 April 2015

Abstract Functionalized magnetic core–shell nanoparticles Fe_3O_4-SiO_2-HMTA are prepared by co-precipitation method and characterized by SEM, TEM, FT-IR, XRD, and VSM. The particles are spherical with an average size of approximately 48 nm. The catalytic activity of these nanoparticles was tested in solvent-free synthesis of coumarin derivatives. The catalyst was readily recycled by the use of an external magnetic field and can be reused four times without significant loss of activity or mass.

Graphical abstract

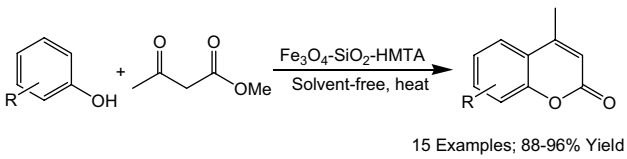

Keywords Magnetically retrievable · Grafting · Silica · Nano-hybrid · Coumarin synthesis · Hexamine · Solvent-free

Introduction

The significant advancement in nanotechnology has led to applications of magnetic nanoparticles (MNPs) in catalysis, environmental protection, energy storage, and biomedicine [1, 2]. The catalytic application of MNPs has attracted increasing attention owing to easy separation from the reaction system by external magnetic field rather than filtration or centrifugation [3]. Uncoated MNPs tend to form aggregates [4]. Silica is often employed as coating material over the surface of iron oxide NPs. The nonmagnetic shell of silica can prevent MNPs from aggregating and agglomerating. The highly porous surface of silica materials has reactive silanol groups that allow covalent immobilization of organic functional groups for the formation of organic–inorganic hybrid nanomaterials [5].

An organic–inorganic hybrid nanomaterial consists of an inorganic support with organic functionalities covalently connected to the framework. Organic–inorganic hybrid nanomaterials can be designed at a molecular level to perform catalysis, adsorption, separation, and drug delivery [6, 7]. Recently, several magnetic organic–inorganic hybrid nanomaterials have been used as heterogeneous catalysts in bromination, nitrile hydration, and oxidation reactions [8–10].

Herein, we report that the Fe_3O_4-SiO_2-HMTA organic–inorganic hybrid nanomaterial can be used as a heterogeneous catalyst and surface modification was carried out by grafting HMTA groups and chloride via formation of covalent bonds to the particle surface. This catalyst for solvent-free synthesis of coumarin derivatives by condensation of phenolic compounds with methyl acetoacetate and could be readily separated from solution via application of an external magnet, allowing straightforward recovery and reuse [11–16].

Electronic supplementary material The online version of this article (doi:10.1007/s13738-015-0652-6) contains supplementary material, which is available to authorized users.

✉ Issa Yavari
yavarisa@modares.ac.ir

[1] Department of Chemistry, Science and Research Branch, Islamic Azad University, Tehran, Iran

[2] Department of Chemistry, Payame Noor University, Tabriz, Iran

Published online: 23 May 2015

Experimental

Materials and methods

Iron (III) chloride hexahydrate ($FeCl_3{\cdot}6H_2O$), iron (II) chloride tetrahydrate ($FeCl_2.4H_2O$), ammonium hydroxide solution ($NH_3.H_2O$, 25 %), tetraethylorthosilicate (TEOS), 3-chloropropyltrimethoxysilane (CPTMS), hexamethylenetetramine (hexamine, HMTA) [17], methyl acetoacetate, phenolic compounds, and solvents were obtained from Merck.

Preparation of the catalyst

Synthesis of magnetite NPs

Magnetite NPs were prepared by chemical co-precipitation method under alkaline condition [18]. Molar ratio of Fe^{2+} and Fe^{3+} salts was maintained at 1:2. In a typical synthesis, $FeCl_3{\cdot}6H_2O$ (5.4 g, 20 mmol) and $FeCl_2{\cdot}4H_2O$ (3.9 g, 20 mmol) were dissolved in water (25 mL) with vigorous stirring. The solution was stirred under N_2 at 80 °C for 1 h. Then, NH_4OH (10 mL) was added and stirred for 2 h. The reaction mixture was cooled to room temperature, and the black powder was collected by an external magnetic field, washed with 50 % aqueous ethanol, and dried under vacuum at 80 °C.

Synthesis of citrate-coated Fe_3O_4 NPs

To obtain the well-dispersed Fe_3O_4 NPs, the prepared MNPs were added to citric acid (10 mL, 0.1 M) with under sonication for 30 min. The reaction was maintained for 12 h at room temperature, and the product was washed several times with water. The obtained citrate-coated MNPs (CMNPs) were separated with external magnetic field. Citric acid was used as a coating agent for colloidal stabilization of MNPs in aqueous solution and to prevent aggregation of MNPs [18].

Synthesis of Fe_3O_4-SiO_2 core–shell NPs

The Fe_3O_4-SiO_2 core–shell NPs were prepared by the growth of a silica layer [19]. Thus, the obtained CMNPs (1.0 g) were added to 10 % aqueous EtOH (20 mL) and the mixture sonicated for 30 min. Under continuous stirring, ammonia solution (5 mL) and tetraethoxyorthosilicate (TEOS, 5 mL) were consecutively added to the reaction mixture. The resulting mixture was stirred under N_2 atmosphere for 12 h at room temperature.

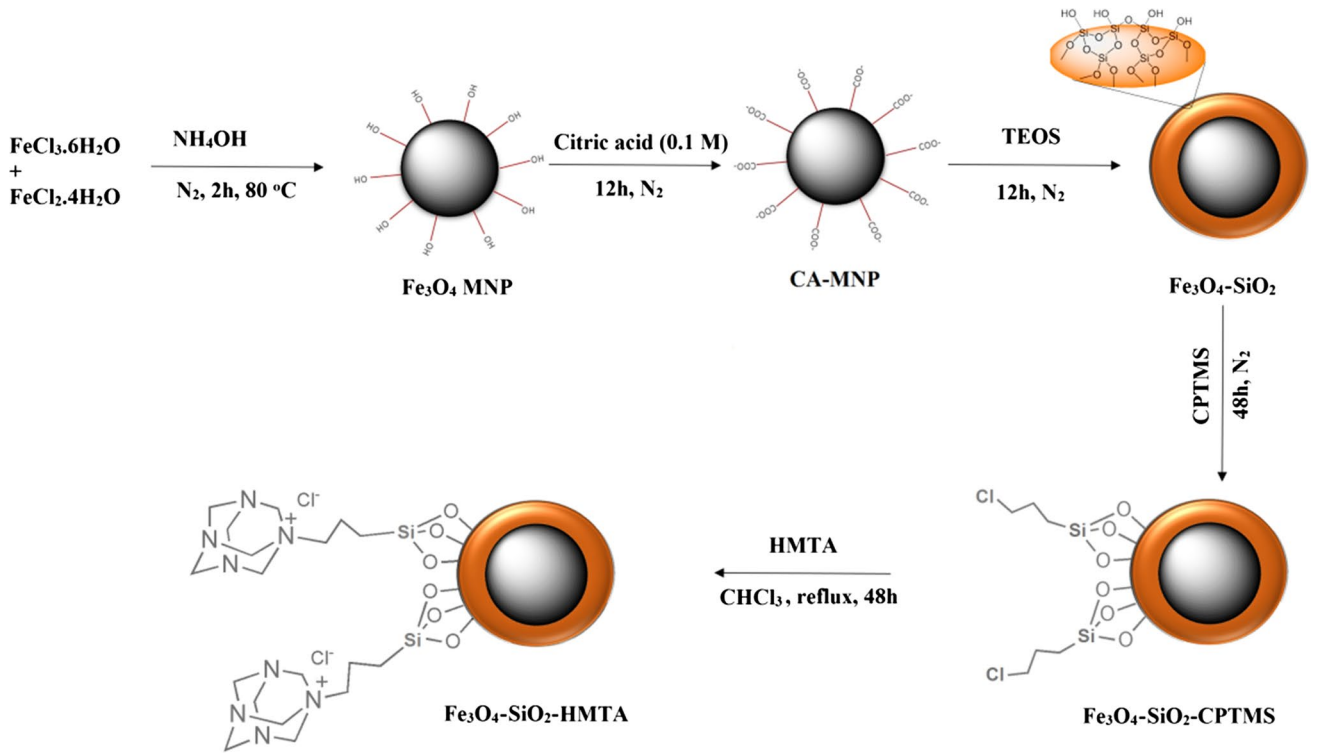

Scheme 1 Preparation of Fe_3O_4-SiO_2-HMTA

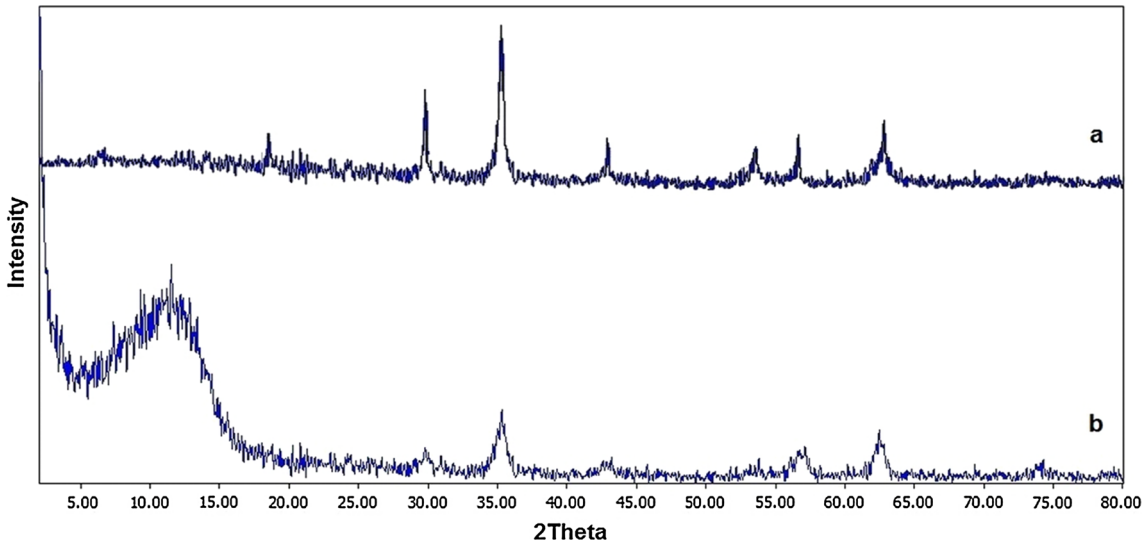

Fig. 1 Powder XRD patterns of **a** Fe_3O_4 and **b** Fe_3O_4-SiO_2-HMTA

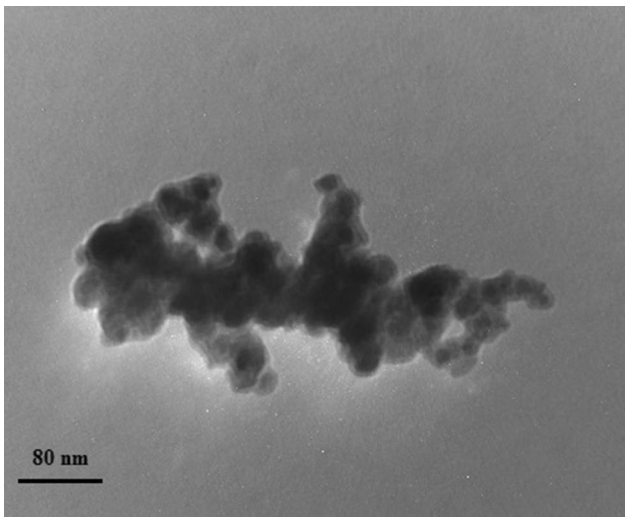

Fig. 2 The TEM image of Fe_3O_4-SiO_2-HMTA

Then, the core–shell NPs were separated by a magnet to eliminate the homogeneous silica nucleus and washed with ethanol.

Synthesis of Fe_3O_4-SiO_2-CPTMS

The obtained MNPs powder were dispersed in MeOH (100 mL), toluene (2 mL), was added to the solution and sonicated for 30 min, then, 3-cloropropyltrimethoxysilane (CPTMS, 2 mL) was added dropwise. After stirring for 48 h under N_2, the mixture was centrifuged, the precipitate was washed with MeOH (3 × 10 mL), and dried under vacuum at 80 °C for 2 h [19].

Synthesis of Fe_3O_4-SiO_2-HMTA

To a solution of hexamine (1.40 g, 10 mmol) in $CHCl_3$ (7 mL), was added Fe_3O_4-SiO_2-CPTMS nanoparticles and the suspension was refluxed for 24 h. Then, the brown solid was washed by $CHCl_3$ and dried under vacuum at 80 °C for 2 h.

Catalyst characterization

Scan electron microscope (SEM) images were obtained using a LEO 1430VP instrument. Transmission electron microscopy (TEM) image was acquired using a Philips EM 208, at 100 kV. FT-IR spectra of the materials were recorded over the range of 400–4000 cm^{-1} region by using a Bruker Tensor 27 FT-IR spectrometer, using a KBr disc made by 1 % sample in 200 mg of spectroscopic-grade KBr. Powder X-ray diffraction (XRD) patterns were recorder in the range of 2°–70° on a Siemens D5000 X-ray Diffractometer, using CuKα radiation ($\lambda = 1.5418$ Å) at 30 kV and 30 mA. The magnetic studies were carried out on a VSM lakeshore 7307 vibrating sample magnetometer.

Typical procedure for the synthesis of coumarin derivatives

A mixture of phenolic compound (1 mmol), methyl acetoacetate (0.1 g, 1 mmol) and Fe_3O_4-SiO_2-HMTA nanomaterial (10 % mol) was stirred at 100 °C for 20 min. Then, the reaction was allowed to cool to room temperature. After completion of reaction, as monitored by TLC, the mixture was diluted with EtOH (2 mL). The catalyst was separated by an external magnet and the product was purified by recrystallization from EtOH.

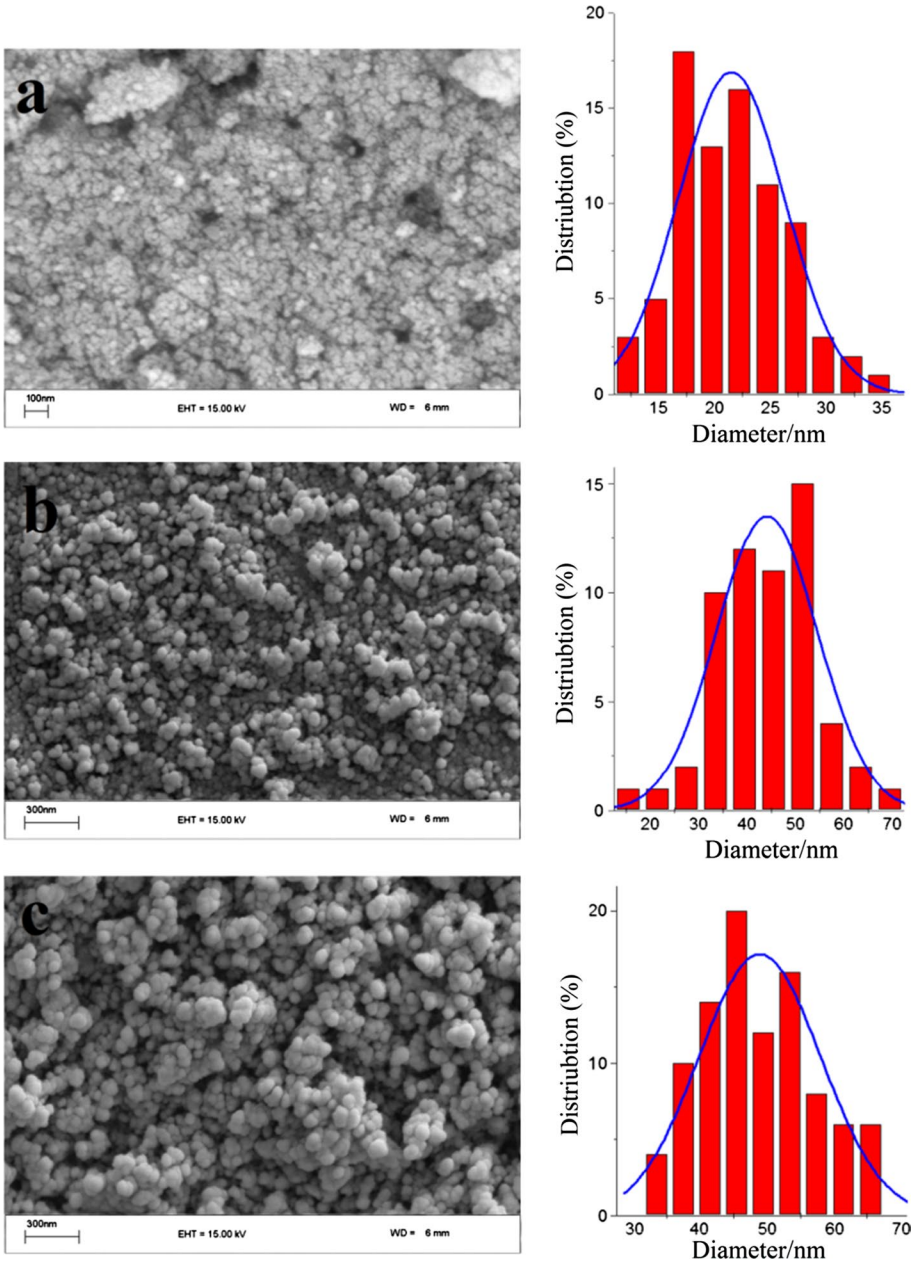

Fig. 3 The SEM images and narrow distribution size diagrams of **a** Fe_3O_4, **b** Fe_3O_4-SiO_2 and **c** Fe_3O_4-SiO_2-HMTA

Results and discussion

Preparation and characterization of the catalyst

The schematic presentation for preparation of Fe_3O_4-SiO_2-HMTA organic–inorganic hybrid nanomaterial is illustrated in Scheme 1. The magnetic nanoparticles were easily prepared via the co-precipitation method. Citric acid was used as a coating agent, covalently attached on the MNPs surface, and made stable colloidal dispersion [15]. The choice of citric acid over other commonly available coating agents is to control the hydrodynamic size and prevent aggregation of MNPs at physiological condition. Coating the magnetic nanoparticles with the silica matrix should be a good solution. Furthermore, the silica hydroxyl groups (Si–OH) were modified by CPTMS groups with covalent bonds. Finally, HMTA was immobilized on the nanoparticle with a covalent bond between silane groups and HMTA.

Structural and compositional characterization

The XRD powder diffraction patterns of Fe_3O_4 and Fe_3O_4-SiO_2 modified by hexamine are shown in Fig. 1. All of the observed diffraction peaks are indexed by the cubic

structure of Fe_3O_4 (PDF: 00-011-0614). As can be seen, the Fe_3O_4-SiO_2 modified by hexamine, the XRD patterns of Fe_3O_4 (Fig. 1a) and Fe_3O_4-SiO_2-HMTA (Fig. 1b) organic–inorganic hybrid nanomaterial were in agreement with that of the standard Fe_3O_4 structure indicated that these particles have phase stability and the structural integrity was preserved. The diffraction peaks at $2\theta = 29.9$, 35.4, 43.1, 53.4, 57.3, 62.4 and 74.1 that correspond to the (2 2 0), (3 1 1), (4 0 0), (4 2 2), (5 1 1), (4 4 0) and (5 3 3) of Fe_3O_4 crystalline structure. A broad diffraction peak near $2\theta = 12°$ is observed in the Fe_3O_4-SiO_2-HMTA organic–inorganic hybrid nanomaterial. This may be attributed to the amorphous SiO_2.

The size of the prepared catalyst was characterized by TEM, which shows the Fe_3O_4-SiO_2-HMTA Fig. 2.

To have a better visual insight into the morphology of Fe_3O_4, Fe_3O_4-SiO_2, Fe_3O_4-SiO_2-HMTA and composite structural changes, scanning electron microscopy images are observed. The diagrams adjacent to Fig. 3a illustrate narrow size distribution of NPs. Figure 3b clearly shows the Fe_3O_4 and Fe_3O_4-SiO_2 NPs with uniform structures. Moreover, as it is shown in Fig. 3c, the Fe_3O_4-SiO_2-HMTA organic–inorganic hybrid nanomaterial has core–shell structure, even after surface modification of Fe_3O_4-SiO_2 NPs with HMTA groups. The mean radii in Fig. 3a are 22.5, 44.6, and 48.7 nm, respectively.

The magnetic properties of Fe_3O_4 were characterized by vibrating sample magnetometer (VSM). The typical room temperature magnetization curves bare Fe_3O_4 (Fig. 4a) and Fe_3O_4-SiO_2-HMTA (Fig. 4a) are shown. The magnetic saturation values of the Fe_3O_4 and Fe_3O_4-SiO_2-HMTA were 59 and 32 emu/g, respectively. Lower magnetic saturation of later nanoparticles could be owing to the existence of nonmagnetic materials on the surface of magnetic nanoparticles.

The FT-IR spectra of (a) Fe_3O_4, (b) Fe_3O_4-SiO_2, and (c) Fe_3O_4-SiO_2-HMTA are shown in Fig. 5. The absorption band at 3438 cm^{-1} in the FT-IR spectrum of Fe_3O_4 nanoparticles (Fig. 5a) is attributed to the stretching vibrations of –OH groups absorbed by Fe_3O_4 nanoparticles. The bands at 1613 and 565 cm^{-1} are assigned to the –OH bending and Fe–O bond vibration, respectively. The broad high-intensity band at 1062 cm^{-1} of Fe_3O_4-SiO_2 (Fig. 5b) is assigned to the Si–O–Si vibration. The bands at 799 and 455 cm^{-1} are assigned to the Si–O–Si symmetric stretch and O–Si–O bending modes, respectively. The bands at 3425, 1630 cm^{-1} correspond to the stretching and bending vibrations of Si–OH [19]. Characteristic bonds at 3000, 2925, 1459, and 1374 cm^{-1} for the organic groups on Fe_3O_4-SiO_2 and $C–N^+$ stretching at 1615 cm^{-1},

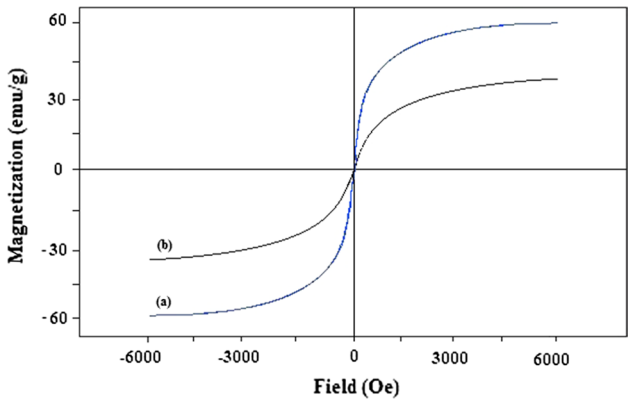

Fig. 4 Magnetization curves obtained by VSM at room temperature for (*a*) Fe_3O_4 MNPs, (*b*) Fe_3O_4-SiO_2-HMTA

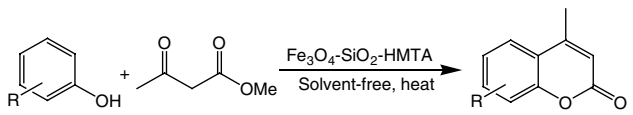

Scheme 2 Preparation of coumarins from phenolic compounds and methyl acetoacetate in the presence of Fe_3O_4-SiO_2-HMTA

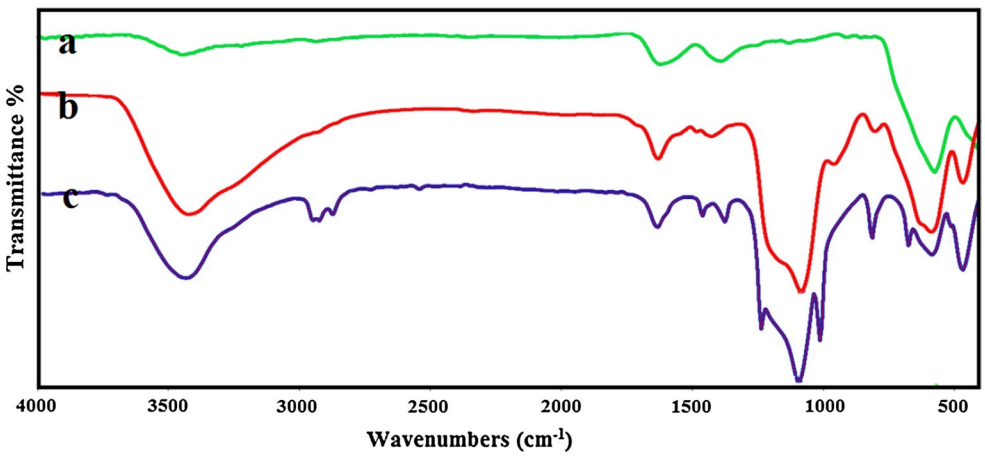

Fig. 5 FT-IR spectra of *a* Fe_3O_4, *b* Fe_3O_4-SiO_2, and *c* Fe_3O_4-SiO_2-HMTA

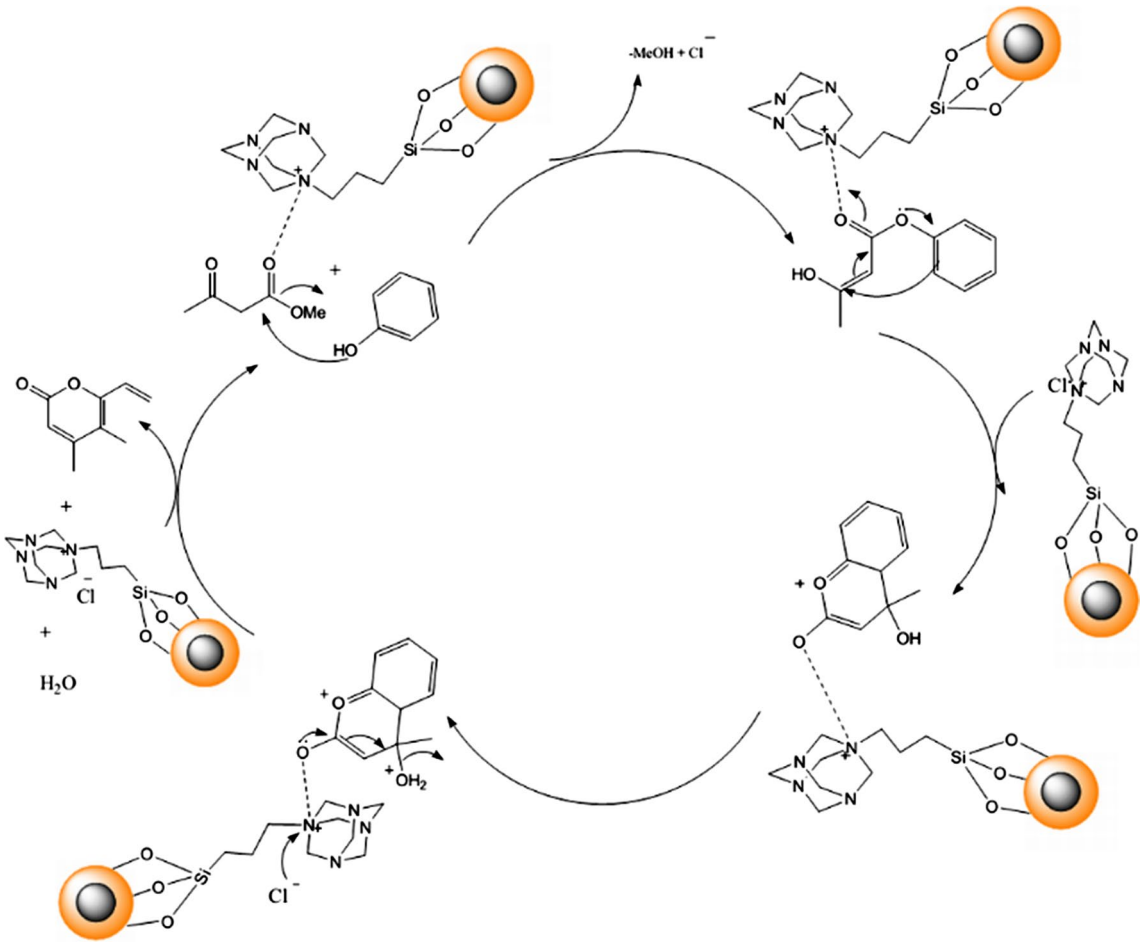

Scheme 3 A plausible mechanism for the synthesis of coumarin on Fe_3O_4-SiO_2-HMTA surface

C–N stretching bonds are at 1009–1233 cm^{-1} are shown in Fig. 5c.

Application of Fe_3O_4-SiO_2-HMTA as nanomagnetic catalyst for synthesis of coumarin derivatives

The catalytic activity of Fe_3O_4-SiO_2-HMTA organic–inorganic hybrid nanomaterial was used as an appropriate heterogeneous acidic catalyst for solvent-free synthesis of coumarin by condensation of phenolic compounds with methyl acetoacetate (Scheme 2).

A plausible mechanism for the synthesis of coumarin on Fe_3O_4-SiO_2 modified by hexamine surface is depicted in Scheme 3.

In order to generalize the scope of reaction, a variety of phenols was subjected for reaction with methyl acetoacetate under the solvent-free optimized reaction conditions, and the results are presented in Table 1. The spectral data and melting points are in good agreement with those reported in literature. The reactions went on well to afford products in good to high yields and short times.

The superiority of the present protocol over reported methods can be seen by comparing our results with those of some recently reported procedures, as shown in Table 2. The synthesis of 4-methyl-2*H*-chromen-2-one was used as a model reaction and the comparison is in terms of mol % of the catalysts, temperature, reaction time, and percentage yields.

Catalyst stability and reusability

The stability of Fe_3O_4-SiO_2-HMTA was tested on the reaction of phenol and methyl acetoacetate. The catalyst was readily recovered by simple magnetic decantation, washed with EtOH and dried at 60 °C for 2 h. The recycled catalyst was used four times with 1–3 % loss of activity or mass (see Table 3).

Table 1 Synthesis of coumarin derivatives catalyzed by Fe_3O_4-SiO_2-HMTA

Entry	Ar-OH	Product	Time (min)	Yield (%)	MP (°C)	
					Observed	Reported (references)
1	Phenol	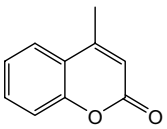	12	96	77–82	79–81 [20]
2	Catechol	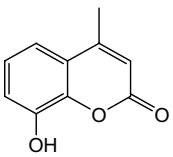	10	90	163–165	161–165 [21]
3	Resorcinol	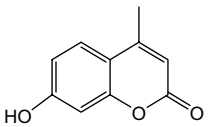	15	93	184–187	182–184 [22]
4	Hydroquinone	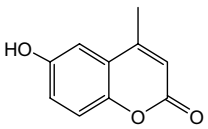	20	91	241–244	241–242 [20]
5	*m*-Cresol	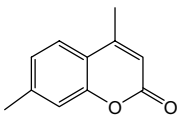	15	90	125–129	130–131 [23]
6	*p*-Cresol	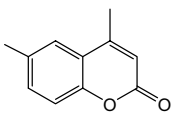	17	90	152–156	150–153 [23]
7	3-Methoxyphenol	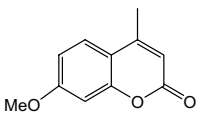	15	89	157–160	158–160 [22]
8	4-Methoxyphenol	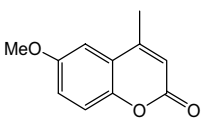	15	88	246–248	240–242 [15]
9	2-Methylresorcinol	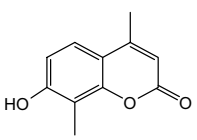	15	95	133–137	137–139 [24]

Table 1 continued

Entry	Ar-OH	Product	Time (min)	Yield (%)	MP (°C)	
					Observed	Reported (references)
10	5-Methylresorcinol	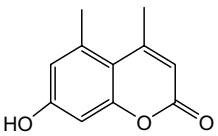	12	89	140–143	141–144 [24]
11	3,5-Dimethylphenol	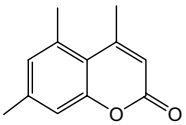	15	92	87–89	88–90 [23]
12	1-Naphthol	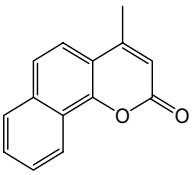	20	89	153–157	154–156 [22]
13	2-Naphthol	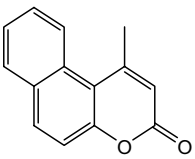	20	89	181–185	182–183 [15]
14	Benzene-1,2,3-triol	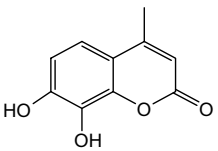	15	93	240–243	238–243 [22]
15	Benzene-1,3,5-triol	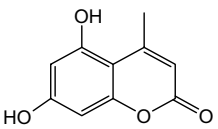	14	90	283–285	289–290 [21]

Table 2 Comparison of the results obtained in this work for 4-methyl-2*H*-chromen-2-one to those reported by other groups

Entry	Catalyst	Reaction conditions	Time	Yield (%)	References
1	Sulphated zirconia	Neat/80 °C	24 h	52	Rodríguez-Domínguez and Krisch [15]
2	[BMIM] [Tf_2N], $FeCl_3$	Neat/70 °C	10 h	77	Karimi and Behzadnia [25]
3	H_3PO_4 imidazolium dihydrogenphosphate	MW heating oven/140 W	25 min	78	Valizadeh et al. [26]
4	$KAl(SO_4)_2{\cdot}12H_2O$	Neat/80 °C	2 h	90	Dabiri et al. [27]
5	$Yb(OTf)_3$	Neat/85 °C	1 h	91	Wang et al. [28]
6	Nano-Fe_3O_4	90 °C	50 min	59	Nasseri and Sadeghzadeh [29]
7	Nano γ-Fe_2O_3	90 °C	50 min	63	Nasseri and Sadeghzadeh [29]
8	Fe_3O_4-DABCO MNP	Solvent-free	50 min	93	Nasseri and Sadeghzadeh [29]
9	Fe_3O_4-SiO_2-HMTA	Solvent-free	12 min	96	This work

Table 3 Recycling of Fe_3O_4-SiO_2-HMTA for synthesis of coumarin by condensation reaction of phenol and methyl acetoacetate

Cycle	Time (min)	Yield (%)
1	12	96
2	12	92
3	15	89
4	20	88

Conclusions

In summary, we have shown that functionalized magnetic core–shell NPs Fe_3O_4-SiO_2-HMTA, prepared by co-precipitation method, is an effective and recyclable catalyst for the synthesis of coumarin derivatives from phenolic compounds and methyl acetoacetate, under solvent-free conditions. Mild reaction conditions, high activity, easy preparation and reusability of the catalyst make the present protocol a green alternative.

References

1. M. Faraji, Y. Yamini, M. Rezaee, J. Iran. Chem. Soc. **7**, 1–37 (2010)
2. G.H. Imanzadeh, A. Zare, A. Khalafi-Nezhad, A. Hasaninejad, A.R. Moosavi-Zare, A. Parhami, J. Iran. Chem. Soc. **4**, 467–475 (2007)
3. F. Shirini, M. Abedini, J. Nanosci, Nanotechnol. **13**, 4838–4860 (2013)
4. S. Pagoti, S. Surana, A. Chauhan, B. Parasar, J. Dash, Catal. Sci. Technol. **3**, 584–588 (2013)
5. S. Chen, J. Feng, X. Guo, J. Hong, W. Ding, Mat. Lett. **59**, 985–988 (2005)
6. A.J. Lan, K.H. Li, H.H. Wu, D.H. Olson, T.J. Emge, W. Ki, M.C. Hong, J. Li, Angew. Chem. Int. Ed. **48**, 2334–2338 (2009)
7. S. Pramanik, C. Zheng, T.J. Emge, J. Li, J. Am. Chem. Soc. **133**, 4153–4155 (2011)
8. H. Erdemi, A. Baykal, E. Karaoğlu, M.S. Toprak, Mat. Res. Bull. **47**, 2193–2199 (2012)
9. V. Polshettiwar, R. Luque, A. Fihri, H. Zhu, M. Bouhrara, J.M. Basset, Chem. Rev. **111**, 3036–3075 (2011)
10. A. Rostami, Y. Navasi, D. Moradi, A. Ghorbani-Choghamarani, Cat. Commun. **43**, 16–20 (2014)
11. I. Yavari, R. Hekmat-Shoar, A. Zonouzi, Tetrahedron Lett. **39**, 2391–2396 (1998)
12. A. Shaabani, R. Ghadari, A. Rahmati, A.H. Rezayan, J. Iran. Chem. Soc. **6**, 710–716 (2009)
13. G. Brufola, F. Fringuelli, O. Piermatti, F. Pizzo, Heterocycles **43**, 1257–1266 (1996)
14. S.K. De, R.A. Gibbs, Synthesis, (8), 1231–1233 (2005)
15. J.C. Rodríguez-Domínguez, G. Kirsch, Synthesis, (11), 1895–1899 (2006)
16. M.S. Manhas, S.N. Ganguly, S. Mukherjee, A.K. Jain, A.K. Bose, Tetrahedron Lett. **47**, 2423–2426 (2005)
17. N. Kaur, D. Kishore, J. Iran. Chem. Soc. **10**, 1193–1228 (2013)
18. S. Srivastava, R. Awasthi, N.S. Gajbhiye, V. Agarwal, A. Singh, A. Yadav, R.K. Gupt, J. Colloid Interface Sci. **359**, 104–111 (2011)
19. Y. Yao, Sh Miao, Sh Yu, L.P. Ma, H. Sun, Sh Wang, J. Colloid Interface Sci. **379**, 20–27 (2012)
20. L.L. Woods, J. Sapp, J. Org. Chem. **27**, 3703–3705 (1962)
21. F. Chavan, B. Madje, J. Bharad, M. Ubale, M. Ware, M. Shingare, N. Shinde, Bull. Cat. Soc. India **7**, 41–45 (2008)
22. S.B. Patil, R.P. Bhat, V.P. Raje, S.D. Samant, Synth. Commun. **36**, 525–531 (2006)
23. A. Russel, J.R. Frye, Org. Synth. **21**, 22–27 (1941)
24. A.S.R. Anjaneyulu, L.R. Row, C.S. Krishna, C. Srinivasulu, Current Sci. **375**, 13–18 (1968)
25. B. Karimi, H. Behzadnia, Cat. Commun. **12**, 1432–1436 (2011)
26. H. Valizadeh, F.M. Kordi, H. Gholipur, M. Amiri, Phosphorus, Sulfur. Silicon Relat. Elem. **184**, 3075 (2009)
27. M. Dabiri, M. Baghbanzadeh, S. Kiani, Y. Vakilzadeh, Monatsh. Chem. **138**, 997 (2007)
28. L. Wang, J. Xia, H. Tian, C. Qian, Y. Ma, Ind. J. Chem. **42B**, 2097 (2003)
29. M.A. Nasseri, S.M. Sadeghzadeh, J. Iran. Chem. Soc. **11**, 27 (2014)